resistance at ca. 15 K. Below this temperature, a sharp decrease of the resistance is observed down to 2 K. Upon heating again the samples exhibit reversible behavior in the low-temperature range, but hysteresis is observed in the insulator regime. The temperature of the resistance maximum is sample dependent (from 9 to 25 K), and this may be due to order–disorder transitions in the cation or subtle changes in the stoichiometry. However, the overall behavior is reproducible and has been observed for more than six samples. This behavior is also reminiscent of that observed at higher temperatures for some samples of the superconducting κ-(BEDT-TTF)$_2$[Cu(NCS)$_2$] phase.[12]

(12) Urayama, H.; Yamochi, H.; Saito, G.; Nozawa, K.; Sugano, T.; Kinoshita, H.; Sato, S.; Oshima, K.; Kawamoto, A.; Tanaka, J. *Chem. Lett.* **1988**, 55–58.

Additional work is in progress so as to better characterize the new molecular metal $(NHMe_3)_{0.5}[Ni(dmit)_2]$ and elucidate its properties (sample dependence, nature of both transitions, pressure effects, etc.). However, these promising preliminary results open a new area of investigation on $(NH_yMe_{4-y})_x[M(dmit)_2]$ systems with different y values as well as with different metals, M; for example, parallel studies on such systems with M = Pd and Pt are underway and will be reported shortly.

Acknowledgment. This work is sponsored by the Programme Interdisciplinaire de Recherche sur les Matériaux (PIRMAT) of CNRS, under ATP Contract Supraconducteurs 88 89N83/0231. C.T. is a postdoctoral fellow, sponsored by the Spanish Consejo Superior de Investigaciones Cientificas (CSIC).

Articles

Structural, Chemical, and Physical Properties of Rare-Earth Metal Rhodium Carbides $LnRhC_2$ (Ln = La, Ce, Pr, Nd, Sm)†

Rolf-Dieter Hoffmann, Wolfgang Jeitschko,* and Ludger Boonk

Anorganisch-Chemisches Institut, Universität Münster, Wilhelm-Klemm-Strasse 8, D-4400 Münster, West Germany

Received March 24, 1989

The title compounds were prepared by arc melting and subsequent annealing. $LaRhC_2$ and $CeRhC_2$ melt congruently, while the others are formed by peritectic reactions. $LaRhC_2$ and $CeRhC_2$ crystallize with a tetragonal structure of space group $P4_3$ (and $P4_1$), which was determined from single-crystal X-ray data of $CeRhC_2$ (a = 392.45 (9) pm, c = 1526.0 (7) pm; R = 0.037 for 692 structure factors and 26 variable parameters). $PrRhC_2$, $NdRhC_2$, and $SmRhC_2$ crystallize with the orthorhombic $CeNiC_2$ type structure, which was refined from single-crystal X-ray data of $SmRhC_2$ (space group $Amm2$, a = 358.91 (6) pm, b = 469.29 (7) pm, c = 656.7 (1) pm; R = 0.027 for 373 F values and 12 variables). The compounds contain C_2 pairs with C–C distances of 139 (2) pm ($CeRhC_2$) and 134 (1) pm ($SmRhC_2$), thus indicating double bonds. The hydrolyses with hydrochloric acid yield mixtures of methane, ethane, propane, and the various isomers of butane, pentane, and hexane but little ($LaRhC_2$) or no ($SmRhC_2$) unsaturated hydrocarbons. $LaRhC_2$ is diamagnetic at room temperature, while the carbides $LnRhC_2$ (Ln = Ce, Pr, Nd) show Curie–Weiss behavior with magnetic moments corresponding to those of the trivalent rare-earth metal ions. $SmRhC_2$ is Van Vleck paramagnetic. The samples of $LaRhC_2$ and $CeRhC_2$ are semiconducting, while those of $PrRhC_2$ and $NdRhC_2$ show metallic behavior. The crystal structures and properties of these carbides are discussed.

Introduction

Because of their importance to the nuclear reactor industry, the ternary systems of the actinoids with transition metals and carbon have been studied for some time, and several ternary carbides were reported.[1] The corresponding rare-earth transition-metal carbides are of interest because of their potential as superconductors and ferromagnets. Their exploration has begun more recently.

These carbides have the structural characteristics of intermetallics with high coordination numbers for all atoms. In the combinations with the early transition metals and in carbides with low carbon content, the carbon atoms are usually isolated from each other, while C_2 pairs are found frequently in ternary carbides with the late transition metals. Thus isolated carbon atoms were found in the structures of $UMoC_2$,[2] URu_3C_{1-x},[3] U_2IrC_2,[4] $Ce_2Ni_{22}C_3$,[5] $Gd_2Fe_{14}C$,[6,7] $LaMn_{11}C_{2-x}$,[8] $Pr_2Mn_{17}C_{2-x}$,[9] $Ho_2Cr_2C_3$,[10]

†Dedicated to Professor Reginald Gruehn on the occasion of his 60th birthday.

(1) Holleck, H. *J. Nucl. Mater.* **1984**, *124*, 129.
(2) Cromer, D. T.; Larson, A. C.; Roof, R. B. Jr. *Acta Crystallogr.* **1964**, *17*, 272.
(3) Holleck, H.; Kleykamp, H. *J. Nucl. Mater.* **1970**, *35*, 158.
(4) Bowman, A. L.; Arnold, G. P.; Krikorian, N. H. *Acta Crystallogr.* **1971**, *B27*, 1067.
(5) Bodak, O. I., Marusin, E. P.; Fundamenskii, V. S.; Bruskov, V. A. *Sov. Phys. Crystallogr.* **1982**, *27*, 657.
(6) Oesterreicher, H.; Spada, F.; Abache, C. *Mater. Res. Bull.* **1984**, *19*, 1069.
(7) Gueramian, M.; Bezinge, A.; Yvon, K.; Muller, J. *Solid State Commun.* **1987**, *64*, 639.

0897-4756/89/2801-0580$01.50/0

Table I. Guinier Powder Patterns of $LaRhC_2$ and $PrRhC_2$[a]

$LaRhC_2$					$PrRhC_2$				
hkl	Q_c	Q_o	I_c	I_o	*hkl*	Q_c	Q_o	I_c	I_o
101	678	681	17	s	011	680	680	17	m
004	681		25		100	738		<1	
103	1018	1018	89	vs	002	914	913	20	m
110	1270	1270	23	m	111	1417	1416	100	vs
111	1312	1314	75	vs	102	1652	1652	24	m
104	1316		100		020	1804	1803	20	m
112	1440	1439	99	vs	013	2507	2507	25	m
113	1652	1653	27	m	120	2542		1	
105	1698	1697	87	vs	022	2718	2719	12	m
114	1950	1950	4	vw	200	2951	2952	12	m
200	2539	2540	8	w	113	3245	3245	6	w
201	2581	2584	65	vs	122	3456	3456	17	m
107	2719	2723	33	s	211	3630	3633	4	vw
008	2723		17		004	3655		<1	
203	2922	2923	21	m	202	3864	3865	6	w
211	3216	3217	4	vw	031	4288	4289	3	vw
204	3219		1		104	4392	4391	12	w
212	3343	3342	32	s	220	4755	4753	11	w
117	3354	3354	5	m	131	5025	5025	17	m
108	3357		18		213	5457	5454	17	m
213	3556	3555	18	vw	024	5459		<1	
214	3854		4		222	5668	5668	10	w
118	3992	3994	4	vw	033	6115	6115	6	vw
109	4080	4081	6	vw	015	6161		7	
215	4237	4235	23	m	124	6196	6197	16	m
207	4623	4621	8	w	204	6605		<1	
216	4705	4705	67	s					
119	4715		11						
221	5120	5117	5	vw					
222	5247	5243	31	m					
217	5257		16						

[a] The diagrams were recorded with Cu $K\alpha_1$ radiation. The Q values are defined by $Q = 100/d^2$ [nm^{-2}]. For the intensity calculations the positional parameters of $CeRhC_2$ and $SmRhC_2$ were used. Very weak reflections with $I \leq 3$ were omitted in the table of $LaRhC_2$. Observed intensities I_o are abbreviated as follows: vs, very strong; s, strong; m, medium; w, weak; vw, very weak.

YCoC,[11] UCr_4C_4,[12] $Tb_2Mn_{17}C_{3-x}$,[13] $U_5Re_3C_8$,[14] Pr_2ReC_2,[15] and UW_4C_4.[16] Isolated carbon atoms together with C_2 pairs occur in the structures of U_2NiC_3,[17] $La_2Ni_5C_3$,[18] $La_{12}Re_5C_{15}$,[19] $Er_{10}Ru_{10}C_{19}$,[20] and $U_2Cr_2C_5$.[16] Solely carbon pairs were found in the structures of $CeNiC_2$[21] and the isotypic compounds $DyCoC_2$[22] and $DyNiC_2$,[22] in $CeCoC_2$[23] and isotypic $NdCoC_2$,[24] in $ScCoC_2$[25] and isotypic $UCoC_2$,[26] in Er_2FeC_4,[27] and in Sc_3CoC_4.[28] We have recently reported on carbides with the $Er_8Rh_5C_{12}$ type structure,[29-31] which occur with the heavy rare-earth elements. In corresponding samples with the light rare-earth metals we have found the title compounds, which also have C_2 pairs. A preliminary account about the structural properties of these carbides was published earlier.[32] The crystal structures of these five carbides have also been reported recently by Tsokol' et al.[33] These authors have determined the structures from single-crystal X-ray data of tetragonal $LaRhC_2$ and from X-ray powder data of orthorhombic $NdRhC_2$. We determined the structures of tetragonal $CeRhC_2$ and orthorhombic $SmRhC_2$, both from single-crystal X-ray data. Thus the two studies supplement each other, although both of our structure refinements are more accurate. Here we give a full account of our structural work. In addition we report on the hydrolyses and on the magnetic and electrical properties of these carbides.

Sample Preparation and Lattice Constants

Starting materials were the rare-earth metals (purity >99.9%), rhodium powder (>99.9%), and graphite (99.5%). Filings of lanthanum and cerium were prepared under paraffin oil. Adherent iron particles were removed by a magnet. The other rare-earth elements were pur-

(8) Jeitschko, W.; Block, G. *Z. Anorg. Allg. Chem.* **1985**, *528*, 61.
(9) Block, G.; Jeitschko, W. *Inorg. Chem.* **1986**, *25*, 279.
(10) Jeitschko, W.; Behrens, R. K. *Z. Metallkde.* **1986**, *77*, 788.
(11) Gerss, M. H.; Jeitschko, W. *Z. Naturforsch. B* **1986**, *41*, 946.
(12) Behrens, R. K.; Jeitschko, W. *Monatsh. Chem.* **1987**, *118*, 43.
(13) Block, G.; Jeitschko, W. *J. Solid State Chem.* **1987**, *70*, 271.
(14) Block, G.; Jeitschko, W. *Monatsh. Chem.* **1988**, *119*, 319.
(15) Block, G.; Jeitschko, W., unpublished results.
(16) Behrens, R. K.; Jeitschko, W. *Z. Kristallogr.* **1988**, *182*, 19.
(17) Gerss, M. H.; Jeitschko, W. *Z. Kristllogr.* **1986**, *175*, 203.
(18) Tsokol', A. O.; Bodak, O. I.; Marusin, E. P. *Sov. Phys. Crystallogr.* **1986**, *31*, 39.
(19) Block, G.; Jeitschko, W. *Z. Kristallogr.* **1987**, *178*, 25.
(20) Hoffmann, R.-D.; Jeitschko, W. *Z. Kristallogr.* **1987**, *178*, 110.
(21) Bodak, O. I.; Marusin, E. P. *Dokl. Akad. Nauk Ukr. S.S.R. Ser. A* **1979**, *12*, 1048.
(22) Jeitschko, W.; Gerss, M. H. *J. Less-Common Metals* **1986**, *116*, 147.
(23) Bodak, O. I.; Marusin, E. P.; Bruskov, V. A. *Sov. Phys. Crystallogr.* **1980**, *25*, 355.
(24) Gerss, M. H.; Jeitschko, W., unpublished research.
(25) Marusin, E. P.; Bodak, O. I.; Tsokol', A. O.; Baivel'man, M. G. *Sov. Phys. Crystallogr.* **1985**, *30*, 340.
(26) Gerss, M. H.; Jeitschko, W. *Mater. Res. Bull.* **1986**, *21*, 209.
(27) Gerss, M. H.; Jeitschko, W.; Boonk, L.; Nientiedt, J.; Grobe, J.; Mörsen, E.; Leson, A. *J. Solid State Chem.* **1987**, *70*, 19.
(28) Tsokol', A. O.; Bodak, O. I.; Marusin, E. P. *Sov. Phys. Crystallogr.* **1986**, *31*, 466.
(29) Hoffmann, R.-D.; Jeitschko, W. *Z. Kristallogr.* **1986**, *174*, 85.
(30) Hoffmann, R.-D.; Jeitschko, W.; Reehuis, M.; Lee, St. *Inorg. Chem.* **1989**, *28*, 934.
(31) Lee, St.; Jeitschko, W.; Hoffmann, R.-D. *Inorg. Chem.*, in press.
(32) Hoffmann, R.-D.; Jeitschko, W. *Z. Kristallogr.* **1988**, *182*, 137.
(33) Tsokol', A. O.; Bodak, O. I.; Marusin, E. P.; Zavodnik, V. E. *Sov. Phys. Crystallogr.* **1988**, *33*, 202.

Table II. Lattice Constants of Rare-Earth Metal Rhodium Carbides with Tetragonal $CeRhC_2$ and Orthorhombic $CeNiC_2$ Type Structure[a]

compd	struct type	a, pm	b, pm	c, pm	V, nm³
$LaRhC_2$	$CeRhC_2$	396.97 (5)	396.97 (5)	1533.3 (4)	0.2416
		398.1 (1)	398.1 (1)	1535.1 (5)	0.2433[b]
$CeRhC_2$	$CeRhC_2$	392.45 (9)	392.45 (9)	1526.0 (7)	0.2350
		393.6 (1)	393.6 (1)	1535 (1)	0.2378[b]
$PrRhC_2$	$CeNiC_2$	368.22 (4)	470.89 (4)	661.70 (6)	0.1147
		368.4 (1)	470.9 (2)	661.9 (2)	0.1148[b]
$NdRhC_2$	$CeNiC_2$	365.03 (4)	470.03 (7)	660.11 (7)	0.1133
		364.8 (1)	469.8 (1)	659.7 (1)	0.1131[b]
$SmRhC_2$	$CeNiC_2$	358.91 (6)	469.29 (7)	656.7 (1)	0.1106
		359.1 (1)	469.5 (1)	656.6 (1)	0.1107[b]

[a] Standard deviations in the positions of the least significant digits are given in parentheses. [b] Data from ref 33.

chased in the form of chips under oil. Prior to the reactions the paraffin oil was washed away by repeated treatment with dried methylene chloride under argon. Stoichiometric mixtures with a weight of about 0.5 g were cold pressed to pellets which were reacted in an arc-melting furnace. For the annealing process in evacuated silica tubes (10–15 days at 900 °C) the samples were wrapped in tantalum foil. While $LaRhC_2$ and $CeRhC_2$ were already present in the arc-melted samples, the other carbides were formed by peritectic reactions during the annealing processes.

The single crystals for the structure determinations were obtained from carbon-deficient samples. In the case of $CeRhC_2$ a sample with about 10% carbon deficiency was used, because the exact composition of this phase was not known at that time. In the case of the incongruently melting carbide $SmRhC_2$ we aimed for a composition where this carbide might be the first crystallization product, and we used a melt of the composition 1:1:1. After arc melting these samples were annealed in a high-frequency furnace for about 20–40 min in water-cooled silica tubes at temperatures slightly below the melting temperature.

The products were characterized by metallography and by scanning electron microscopy. Energy dispersive X-ray fluorescence analyses did not reveal any impurity elements heavier than magnesium. Guinier powder diagrams were recorded by using α-quartz (a = 491.30 pm, c = 540.46 pm) as standard. Indices could be assigned on the basis of the cells found by the single-crystal investigations. The identifications of the diffraction lines were facilitated by intensity calculations[34] using the positional parameters of the refined structures. As examples, the evaluations of the powder patterns of $LaRhC_2$ and $PrRhC_2$ are shown in Table I. The lattice constants (Table II) were refined by least-squares fits.

Chemical Properties

The ternary rhodium carbides $LnRhC_2$, especially the coarse-grained samples, are stable in air for periods of several months. The hydrolysis with diluted hydrochloric acid proceeded at a much smaller rate than it did with $Er_8Rh_5C_{12}$.[30] A sample of $SmRhC_2$ was hydrolyzed in moderately diluted (1:1) hydrochloric acid at about 60 °C. The emerging gaseous products were analyzed in a gas chromatograph with a flame ionization detector. Besides hydrogen (which was not measured) the following products were determined (in wt %): 34 CH_4, 36 C_2H_6, 12 C_3H_8, 14 n-C_4H_{10}, 2 n-C_5H_{12}, and traces of i-C_4H_{10}, i-C_5H_{12}, and various isomers of hexane. A similar result was obtained with a sample of $LaRhC_2$ which was hydrolyzed at room temperature in 2 N hydrochloric acid. The small amounts of the emerging hydrocarbons (using hydrogen developed at the sample as a carrier gas) caused the gas chromatographic analysis to be less sensitive: 18 CH_4, 53 C_2H_6, 3 C_2H_4, 11 C_3H_8, 12 n-C_4H_{10}, and traces of C_2H_2, C_3H_6, and n-C_5H_{12}. Thus, surprisingly, no unsaturated hydrocarbons were detected in the products of $SmRhC_2$ and very little for $LaRhC_2$, even though the carbon atoms in the two (different) structures form C_2 pairs with C–C bond distances typical for double bonds. These results are similar to those obtained with $Er_8Rh_5C_{12}$.[30] In contrast, large amounts of unsaturated hydrocarbons were detected in the hydrolysis products of U_2NiC_3,[17] $UCoC_2$,[26] Y_2FeC_4,[27] and Er_2FeC_4.[27]

Table III. Magnetic Properties of $RRhC_2$ (R = La–Nd, Sm)[a]

compd	μ_{exp}, μ_B	μ_{eff}, μ_B	θ, K	type of magnetism
$LaRhC_2$				diamagnetic
$CeRhC_2$	2.4 (1)	2.54	−14 (2)	antiferromagnetic?
$PrRhC_2$	3.6 (1)	3.58	−13 (3)	antiferromagnetic?
$NdRhC_2$	3.7 (1)	3.62	0 (2)	ferro or antiferro?
$SmRhC_2$	1.62 (2)	1.66		Van Vleck paramagnetic

[a] The experimentally determined effective magnetic moments per formula unit μ_{exp} are compared with the theoretical effective moments μ_{eff} for the trivalent rare-earth metal ions. The Weiss constants θ were obtained by linear extrapolation of the $1/\chi$ vs T plots. Estimated error limits in the position of the last digit are listed in parentheses.

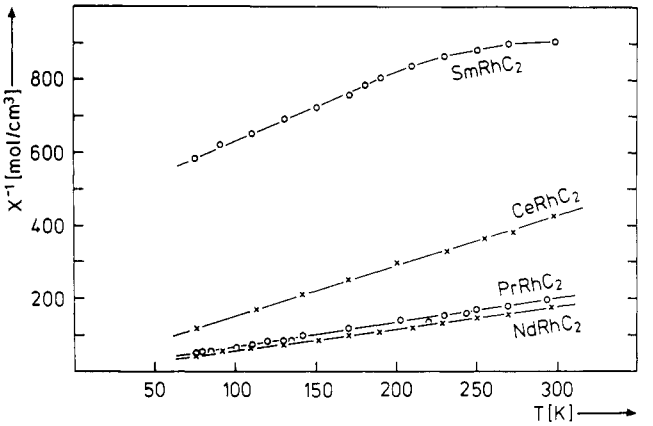

Figure 1. Reciprocal magnetic susceptibilities of the carbides $LnRhC_2$ (Ln = Ce, Pr, Nd, and Sm) as a function of temperature.

Physical Properties

The magnetic susceptibilities of the five carbides were determined with a Faraday balance as described earlier.[35] Samples of about 10–20 mg were measured between 70 and 300 K. The results are summarized in Table III. The sample of $LaRhC_2$ was diamagnetic at room temperature ($\chi = -0.02 \times 10^{-3}$ cm³/mol) and became weakly paramagnetic at lower temperatures ($\chi = +0.06 \times 10^{-3}$ cm³/mol at 98 K). In view of the semiconductivity of this compound, we conclude it to be diamagnetic. The increasing paramagnetism of the sample with lower temperatures can be ascribed to paramagnetic impurities.

The Ce, Pr, and Nd compounds show Curie–Weiss behavior (Figure 1). The experimentally determined effective magnetic moments μ_{exp} agree within the error limits with those of the trivalent rare-earth metal ions calculated from the relation $\mu_{eff} = g[J(J+1)]^{1/2}$. The negative paramagnetic Curie temperatures of the Ce and Pr com-

(34) Yvon, K.; Jeitschko, W.; Parthé, E. *J. Appl. Crystallogr.* **1977**, *10*, 73.

(35) Jeitschko, W.; Reehuis, M. *J. Phys. Chem. Solids* **1987**, *48*, 667.

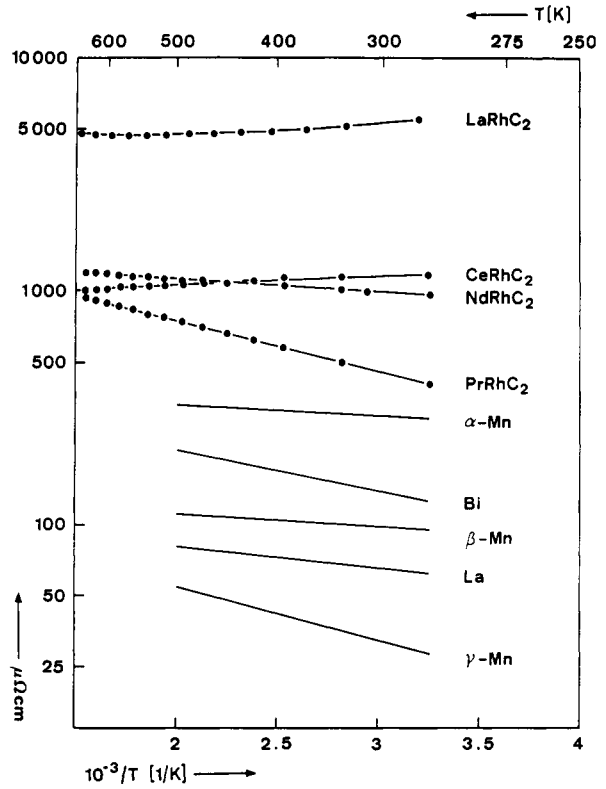

Figure 2. Resistivities of $LaRhC_2$, $CeRhC_2$ (both with $CeRhC_2$ type structure), $PrRhC_2$, and $NdRhC_2$ ($CeNiC_2$ type) as a function of temperature. The absolute values are estimated to be correct only within a factor of 3. For comparison the specific resistivities of some metals are also plotted.

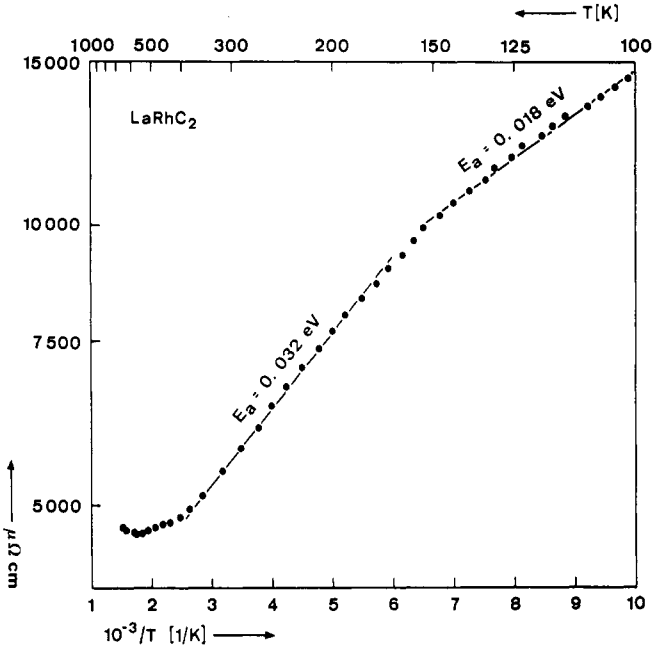

Figure 3. Resistivity of semiconducting $LaRhC_2$. The activation energies E_a were calculated from the linear portions of the log ρ vs $1/T$ plot.

pound are compatible with antiferromagnetic or ferrimagnetic order at lower temperatures. Our experimental setup was not suited to verify this.

The susceptibility of the Sm compound is typical for a Van Vleck ion. The theoretical effective moment of $\mu_{eff} = 1.66\ \mu_B$ calculated from Van Vleck's formula[36] for $T = 300$ K with a screening constant of $\sigma = 34$ agrees well with the experimentally determined magnetic moment $\mu_{exp} = 1.62\ (\pm 0.02)\ \mu_B$ calculated from the relation $\mu_{exp} = 2.83(\chi T)^{1/2}\ \mu_B$.

The electrical conductivities of several carbides were determined with a four-probe technique as a function of temperature. Irregularly shaped pieces of the crushed arc melted, and annealed buttons with a size of about $0.5 \times 0.5 \times 1$ mm^3 were contacted with four copper filaments by using a well-conducting silver epoxy cement. A constant alternating current was applied at two contacts, while the voltage difference was measured between the other contacts. Because of the irregular shapes of the samples the absolute values of the conductivities are estimated to be correct only within a factor of 3. The relative values for one sample at different temperatures are much more reliable. Figure 2 shows the results. For comparison the specific resistivities of some metals taken from the literature[37] are also plotted. The electrical resistivities of the two $CeNiC_2$ type carbides $PrRhC_2$ and $NdRhC_2$ increase with increasing temperature, thus indicating metallic behavior. The resistivities of $LaRhC_2$ and $CeRhC_2$ (both with $CeRhC_2$ type structure), however, show the inverse behavior as is typical for semiconductors. A second sample of $LaRhC_2$ was measured over a larger temperature range (Figure 3). From the slopes of the two linear portions of the log ρ vs $1/T$ plot we calculated the activation energies E_a according to the equation $\rho = \rho_0 \exp(E_a/2kT)$. The values of $E_a = 0.018$ eV and $E_a = 0.032$ eV thus obtained are very small and probably correspond to impurity levels, while the intrinsic gap may be larger.

Some words of caution seem to be appropriate at this point. The semiconducting behavior of the La and Ce compounds and the metallic conductivity of the Pr and Nd compounds correlate with the different structure types and the diamagnetism of the La compound. However, the electrical conductivity could be dominated by foreign material at the grain boundaries and may be different in the La and Ce compounds which melt congruently while the other carbides are formed by peritectic reactions. Metallographic examinations showed that the La and Ce samples consist of large grains with no visible second phase material at the grain boundaries (There were minor inclusions of second-phase material within the grains, which should not cause problems with the conductivity measurements. These impurities were not visible on the Guinier films.) The Guinier films of the annealed samples of $PrRhC_2$ and $NdRhC_2$ used for the electrical conductivity measurements showed minor amounts (about 10%) of the cubic Laves phases $PrRh_2$[38] and $NdRh_2$,[39] which are certainly metallic conductors. Metallographic examination of the $NdRhC_2$ samples showed that this second-phase material was present in well-crystallized grains and not in any visible amounts at the grain boundaries of the ternary carbide. Nevertheless, in view of the relatively low absolute values of the electrical conductivities of $PrRhC_2$ and $NdRhC_2$, we hold the semiconducting behavior of $LaRhC_2$ and $CeRhC_2$ to be better established than the metallic behavior of the other carbides.

Crystal Structures of $CeRhC_2$ and $SmRhC_2$

The single crystals of $CeRhC_2$ and $SmRhC_2$ used for the structure determinations had been grown in the carbon-

(36) Van Vleck, J. H. *The Theory of Electric and Magnetic Susceptibilities*; Oxford University Press: London, 1932; p 248.
(37) Landolt-Börnstein, *Zahlenwerte und Funktionen*, 6th ed.; Springer: Berlin, 1959; Vol. II/6.

(38) Compton, V. B.; Matthias, B. T. *Acta Crystallogr.* **1959**, *12*, 651.
(39) Singh, P. P.; Raman, A. *Met. Trans.* **1970**, *1*, 233.

deficient samples, which were heat treated slightly below the melting points as described before. The crystals were isolated from the samples by selective hydrolyses which attacked the material at the grain boundaries faster than the crystals of the ternary carbides.

The crystals were investigated in Buerger and Weissenberg cameras. Those of $CeRhC_2$ had the Laue symmetry $4/m$. The only extinction condition (reflections $00l$ were observed only with $l = 4n$) led to the two enantiomorphic space groups $P4_1$ (no. 76) and $P4_3$ (no. 78). Crystals of both space groups can be expected in a polycrystalline sample. The structure refinements showed that the crystal used for the structure determination had space group $P4_3$. With $Z = 4$ formula units/cell the calculated density is 7.55 g/cm^3. The isotypy of $SmRhC_2$ with $CeNiC_2$[21] was recognized at an early stage of our investigation. The structure determination confirmed the space group $Amm2$ (no. 38). With $Z = 2$ formula units for the centered cell the calculated density is 8.33 g/cm^3.

Intensity data were recorded on a four-circle diffractometer at room temperature with graphite-monochromated Mo Kα radiation, a scintillation counter, and a pulse-height discriminator. Background scans were taken at both ends of each $\theta/2\theta$ scan. The scanning rates were optimized by fast prescans. Empirical absorption corrections were made from ψ-scan data. The crystal of $CeRhC_2$ (with corresponding values for $SmRhC_2$ in parentheses) had the dimensions $7 \times 8 \times 20$ μm^3 ($7 \times 10 \times 20$ μm^3). The linear absorption coefficient is μ(Mo Kα) = 260 cm^{-1} (167 cm^{-1}). The ratio of the highest to the lowest transmission was 1.08 (1.18). A total of 2490 (1794) reflections was recorded in three octants (the whole sphere) of the reciprocal lattice up to $2\theta = 65°$ (84°). The data were averaged, and reflections with structure factors smaller than 3 standard deviations were omitted; 692 (373) F values remained, which were used for the structure determinations. The inner R value was $R_i = 0.033$ (0.048).

The structure of $CeRhC_2$ was determined from Patterson and difference Fourier analyses. A full-matrix least-squares program supplied by the Enraf-Nonius company was used to refine the structures. The atomic scattering factors[40] were corrected for anomalous dispersion.[41] Weights were assigned according to the counting statistics, and a parameter accounting for the secondary extinction was refined and applied to the calculated structure factors. For both structures a series of least-squares cycles was run with simultaneous refinement of the occupancy and thermal parameters (with constant scale factors). The occupancy factors were as follows (in percent with standard deviations in the place value of the last quoted digit): Ce, 100.5 (2); Rh, 99.2 (3); C(1), 89 (4); C(2), 88 (4); Sm, 99.4 (2); Rh, 101.7 (3); C, 102 (2). Thus all occupancy parameters had the ideal values within 6 standard deviations. Even though at first sight the carbon atoms in $CeRhC_2$ have relatively low occupancy parameters, they are within only 3 standard deviations of their ideal values. Thus we can assume that both compounds are thermodynamically stable at their ideal compositions, especially also if we consider that the crystals for the structure determination were grown at high temperature from carbon-deficient samples. We therefore considered the least-squares refinements with the ideal occupancy values as the final ones.

Since both structures are noncentrosymmetric, we also refined their enantiomeric forms by changing the hkl indices to $\bar{h}\bar{k}\bar{l}$. For the structure of $CeRhC_2$ this also necessitates the change from space group $P4_3$ to $P4_1$. The resulting conventional residuals were both higher (R = 0.049 for both structures) than the ones for the correct polarity. These were $R = 0.037$ ($R_w = 0.029$) for $CeRhC_2$ (692 structure factors, 26 variable parameters) and $R = 0.027$ ($R_w = 0.023$) for $SmRhC_2$ (373 F values, 12 variables). The atomic parameters and interatomic distances are listed

(40) Cromer, D. T.; Mann, J. B. *Acta Crystallogr.* **1968**, *A24*, 321.
(41) Cromer, D. T.; Liberman, D. *J. Chem. Phys.* **1970**, *53*, 1891.

Table IV. Atomic Parameters of $CeRhC_2$ and $SmRhC_2$[a]

$CeRhC_2$

atom	$P4_3$	x	y	z	B[b]
Ce	4a	0.3485 (2)	0.3517 (2)	0[c]	0.343 (8)
Rh	4a	0.1480 (3)	0.1533 (3)	0.59400 (7)	0.63 (1)
C(1)	4a	0.145 (5)	0.165 (4)	0.4605 (8)	0.9 (2)
C(2)	4a	0.150 (6)	0.647 (6)	0.637 (1)	1.7 (3)

$SmRhC_2$ ($CeNiC_2$ Type Structure)

atom	$Amm2$	x	y	z	B[b]
Sm	2a	0	0	0[c]	0.322 (7)
Rh	2b	$^1/_2$	0	0.6243 (2)	0.49 (1)
C	4e	$^1/_2$	0.143 (2)	0.315 (1)	0.5 (1)

[a] Standard deviations in the least significant digit are given in parentheses. [b] The last column contains the isotropic B value of the carbon positions and the equivalent isotropic B value (×100 in units of nm^2) of the anisotropic thermal parameters of the metal atom positions. [c] Parameter held constant to pin the origin of the cell.

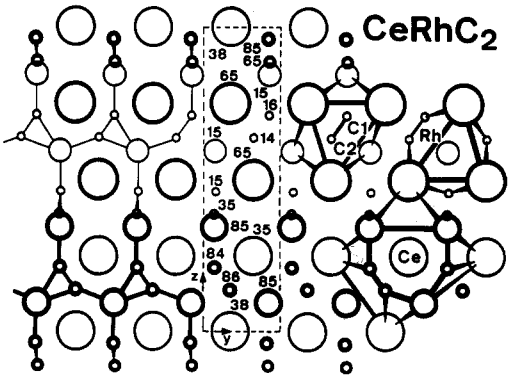

Figure 4. Crystal structure of $CeRhC_2$. Heavy and light circles correspond to the heights of the atoms in the projection direction (in hundredths of the translation period a). On the left-hand side the bonds within the $[RhC_2]^{3-}$ polyanion are emphasized. The right-hand side shows the coordination polyhedra.

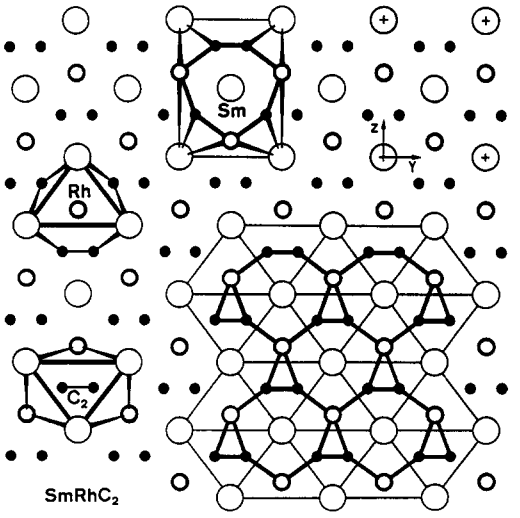

Figure 5. Crystal structure and coordination polyhedra of the $CeNiC_2$ type structure of $SmRhC_2$. The two-dimensionally infinite network of rhodium and carbon atoms is indicated by heavy lines in the lower right-hand corner. The samarium atoms are above and below at $x = 0$.

Table V. Interatomic Distances (picometers) and Selected Interatomic Angles (degrees) in $CeRhC_2$ and $SmRhC_2$[a]

Ce–1C(1)	278 (2)	Sm–4C	274.1 (7)	
Ce–1C(1)	281 (2)	Sm–4C	281.9 (7)	
Ce–2C(2)	286 (2)	Sm–2Rh	305.1 (1)	
Ce–1C(1)	287 (2)	Sm–4Rh	306.5 (3)	
Ce–2C(2)	287 (2)	Sm–2Sm	358.9 (1)	
Ce–1C(1)	290 (2)	Sm–4Sm	403.6 (1)	
Ce–1Rh	310.3 (2)			
Ce–1Rh	312.0 (2)			
Ce–1Rh	312.8 (2)			
Ce–1Rh	314.5 (2)			
Ce–2Rh	317.8 (1)			
Ce–4Ce	392.5 (1)			
Ce–2Ce	399.2 (1)			
Rh–1C(1)	204 (1)	Rh–2C	209.3 (9)	
Rh–1C(2)	204 (2)	Rh–2C	213.9 (9)	
Rh–1C(2)	209 (2)	Rh–2Sm	305.1 (1)	
Rh–1C(1)	213 (1)	Rh–4Sm	306.5 (1)	
Rh–1Ce	310.3 (2)			
Rh–1Ce	312.0 (2)			
Rh–1Ce	312.8 (2)			
Rh–1Ce	314.5 (2)			
Rh–2Ce(1)	317.8 (1)			
C(1)–1C(2)	139 (2)	C–1C	134 (1)	
C(1)–1Rh	204 (1)	C–1Rh	209.3 (9)	
C(1)–1Rh	213 (1)	C–1Rh	213.9 (9)	
C(1)–1Ce	278 (2)	C–2Sm	274.1 (7)	
C(1)–1Ce	281 (2)	C–2Sm	281.9 (7)	
C(1)–1Ce	287 (2)			
C(1)–1Ce	290 (2)			
C(2)–1C(1)	139 (2)			
C(2)–1Rh	204 (2)			
C(2)–1Rh	209 (2)			
C(2)–2Ce	286 (2)			
C(2)–2Ce	287 (2)			
C(1)–Rh–C(2)	38.5 (6)	C–Rh–C	36.5 (3)	
C(1)–Rh–C(2)	107.3 (7)	C–Rh–C	106.5 (3)	
C(1)–Rh–C(2)	104.7 (7)	C–Rh–C	108.5 (3)	(2×)
C(1)–Rh–C(2)	109.5 (7)	C–Rh–C	145.0 (5)	(2×)
C(1)–Rh–C(1)	147.9 (7)			
C(2)–Rh–C(2)	143.2 (6)			
Rh–C(1)–Rh	147 (1)	Rh–C–Rh	145.0 (5)	
Rh–C(1)–C(2)	69 (1)	Rh–C–C	71.8 (5)	
Rh–C(1)–C(2)	143 (1)	Rh–C–C	143.3 (7)	
Rh–C(2)–Rh	143 (1)			
Rh–C(2)–C(1)	72 (1)			
Rh–C(2)–C(1)	145 (1)			

[a] All distances shorter than 440 pm (Ce–Ce, Sm–Sm, Ce–Rh, Sm–Rh), 355 pm (Rh–Rh, Ce–C, Sm–C), and 320 pm (Rh–C, C–C) are listed. Of the interatomic angles only those between the strongly bonded atoms within the polyanions are given. Standard deviations, computed from those of the lattice constants and the positional parameters, are given in parentheses in the position of the least significant digit.

in Tables IV and V. The crystal structures and coordination polyhedra are shown in Figures 4 and 5. The tables with the anisotropic thermal parameters of the metal atoms and the observed and calculated structure factors are available as supplementary material.

Discussion

The tetragonal crystal structure of $LaRhC_2$ and $CeRhC_2$ is closely related to the orthorhombic $CeNiC_2$ and monoclinic $CeCoC_2$ type structures which occur for the ternary cobalt and the other rhodium carbides with this composition (Figure 6). All these structures may be thought of as being composed of trigonal prisms of rare-earth metal atoms, which are packed in different ways (Figure 7). The prisms are filled by equal amounts of transition-metal atoms (T) and C_2 pairs. Considering the large differences in electronegativities the rare-earth metal atoms may be considered to have donated their valence electrons to the

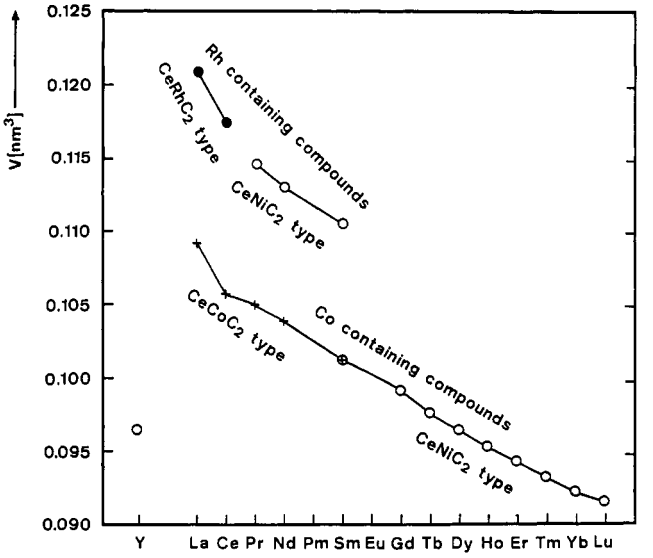

Figure 6. Cell volumes of rare-earth metal cobalt and rhodium carbides with $CeRhC_2$, $CeNiC_2$, and $CeCoC_2$ type structure. For comparison only half the cell volumes are plotted for the $CeRhC_2$ and $CeCoC_2$ type carbides. The data for the cobalt containing carbides are from ref 22.

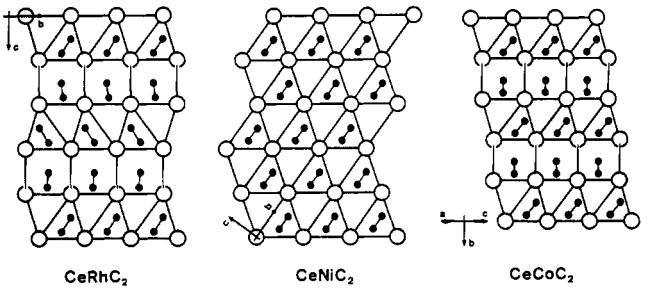

Figure 7. Structural relationships of the three structure types $CeRhC_2$, $CeNiC_2$, and $CeCoC_2$. The three structures may be considered to be composed of trigonal prisms of the Ce atoms (large circles) which are stacked in different ways. Half of these prisms contain the C_2 pairs, the other half the transition-metal atoms, which are not shown.

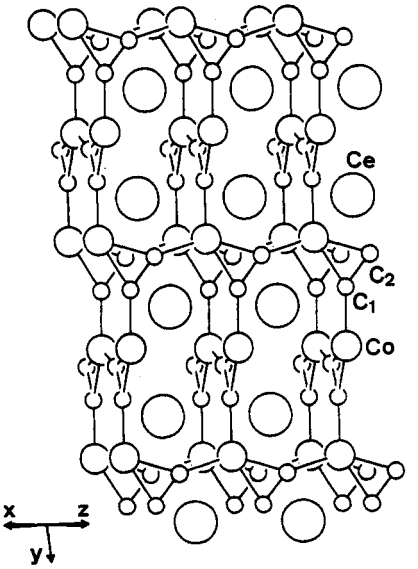

Figure 8. Crystal structure of $CeCoC_2$. The three-dimensionally infinite network of the $(CoC_2)^{3-}$ polyanion is emphasized.

$(TC_2)^{3-}$ polyanions. These polyanions form two-dimensionally infinite sheets in the $CeNiC_2$ type structure (Figure 5), while they form three-dimensional networks in the $CeRhC_2$ (Figure 4) and $CeCoC_2$ (Figure 8) structures.

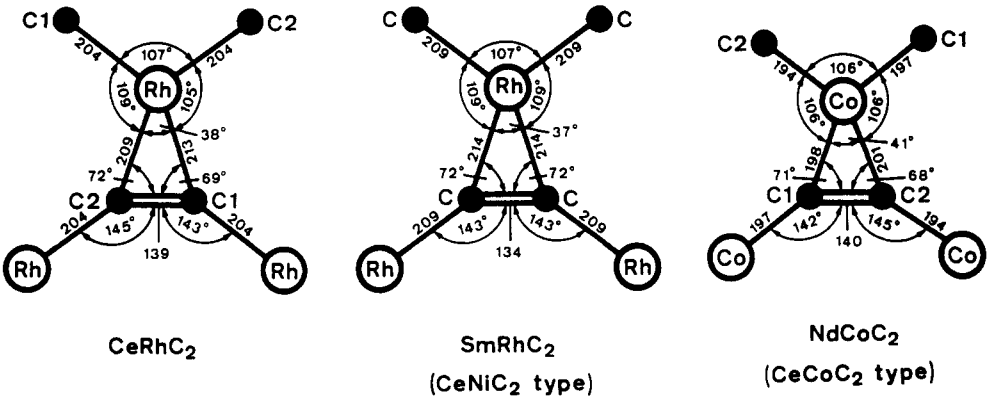

Figure 9. Near-neighbor environments within the polyanions of three carbides RTC_2 with three different structure types. Although the T and C atoms form different infinite two- and three-dimensional nets, the shown seven-atom units are all planar. The interatomic distances are in picometers.

From Figure 6 we conclude that the cerium atoms in $CeRhC_2$ are trivalent (a much smaller cell volume would be expected for a Ce^{IV} compound). Thus the differences in the near-neighbor environments of $CeRhC_2$ and $SmRhC_2$ can be ascribed to the different sizes of the Ce and Sm atoms. The numbers and kinds of nearest neighbors are the same in both structures (Table V). The largest differences in interatomic distances occur for the shortest (nonbonding) R–R distances: 392.5 pm in $CeRhC_2$ vs 358.9 pm in $SmRhC_2$. This may well be the most important reason for the change in structure. There are no bonding Rh–Rh interactions in either structure. The average Ce–Rh distance (314.2 pm) is slightly greater than the average Sm–Rh distance (305.8 pm). This difference is about the same as the difference in the ionic radii (111 pm for Ce^{3+} and 104 pm for Sm^{3+}) and much smaller than the difference in the metallic radii for coordination number 12 (181 pm for Ce vs 166 pm for Sm).

The positions of the light carbons atoms have relatively large standard deviations of the order of 1–2 pm. However, since each C_2 pair is surrounded by three Rh atoms (Figure 9), the *average* Rh–C bond distance is more reliable. Interestingly, these distances are greater in $SmRhC_2$ (which has the smaller cell volume per formula unit) than in $CeRhC_2$: 211.6 vs 207.5 pm. Thus the carbon atoms are more strongly bonded to the Rh atoms in $CeRhC_2$ than in $SmRhC_2$. Since the total "bond strength" of a carbon atom in the two structures may be considered to be equal, this correlates with the shorter C–C distance of 134 pm in $SmRhC_2$ vs 139 pm in $CeRhC_2$. Both distances are close to a C–C double bond (135 pm in C_2H_4). This is not reflected by the hydrolyses products. The hydrolyses of such ternary carbides are complex heterogeneous processes.[24] To our knowledge only Al_4C_3 and CaC_2 give pure gaseous products (CH_4 and C_2H_2, respectively).

The diamagnetism of $LaRhC_2$ and the fact that the other $RRhC_2$ carbides have magnetic moments that correspond to those of the R^{3+} ions indicate that the $(RhC_2)^{3-}$ polyanions are magnetically saturated. The increase in the electrical conductivity with temperature as observed for our samples of $LaRhC_2$ and $CeRhC_2$ even suggests a bandgap between occupied bonding and unoccupied antibonding states.[31,42] In the absence of band structure calculations one may speculate about the change from the semiconducting behavior of the La and Ce compound to the metallic behavior of the other $LnRhC_2$ carbides. This change could be due to the decrease in the electropositivity (and in the gradual closing of the bandgap) in the direction from La and Ce to Pr, Nd, Sm, and/or it could be due to the structural change with the differences in the Rh–C and C–C bonding as discussed above. For a more thorough discussion of the chemical bonding of these carbides, electrical conductivity data established from measurements of single crystals would be desirable. It is unfortunate that today the art of growing single crystals is much less advanced than the science of structure determination. Professor Reginald Gruehn, to whom this paper is dedicated, is contributing to close this gap.

Acknowledgment. We are indebted to Th. Vomhof for the magnetic susceptibility measurements. Dr. M. H. Möller and U. Rodewald collected the single-crystal diffractometer data. K. Wagner characterized our samples with a scanning electron microscope. We also want to thank Prof. J. Grobe and his co-workers for their help and advice with the gas chromatographic analyses. Dr. R. Schwarz (Degussa AG) and Dr. G. Höfer (Heraeus Quarzschmelze) have both supported our work with their generous supply of rhodium metal and silica tubes. The arc-melting furnace was provided by the Deutsche Forschungsgemeinschaft, and relevant chemical literature was purchased by the Fonds der Chemischen Industrie.

Registry No. La, 7439-91-0; Ce, 7440-45-1; Pr, 7440-10-0; Nd, 7440-00-8; Sm, 7440-19-9; Rh, 7440-16-6; $LaRhC_2$, 115805-13-5; $CeRhC_2$, 53262-56-9; $PrRhC_2$, 115805-11-3; $NdRhC_2$, 115805-12-4; $SmRhC_2$, 115710-23-1; CH_4, 74-82-8; C_2H_6, 74-84-0; C_3H_8, 74-98-6; n-C_4H_{10}, 106-97-8; n-C_5H_{12}, 109-66-0; i-C_4H_{10}, 75-28-5; i-C_5H_{12}, 78-78-4; C_2H_2, 74-86-2; C_3H_6, 115-07-1; C_2H_4, 74-85-1; graphite, 7782-42-5; hexane, 110-54-3.

Supplementary Material Available: Tables of the thermal ellipsoid parameters for the atoms of $CeRhC_2$ and $SmRhC_2$ (1 page) and of the observed and calculated structure factors for $CeRhC_2$ and $SmRhC_2$ (6 pages). Ordering information is given on any current masthead page.

(42) Li, J.; Hoffmann, R. *Chem. Mater.* **1989**, *1*, 83.